Optical Interferometric Characterization of Nonlinear Optical Polymer Thin Films

J. W. Wu

Department of Physics, Ewha Womans University, Seoul 120-750, Korea
[jwwu@mm.ewha.ac.kr]

ABSTRACT

The linear electro-optic (EO) effect is one of the second-order nonlinear optical effects existing in a noncentrosymmetric macroscopic system. In a polymer thin film, the noncentrosymmetry is achieved by electric field poling. The magnitude of the linear EO response is determined through the orientational distribution function of hyperpolarizable molecular dipoles. The relation between the linear EO coefficient and the second-order nonlinear optical susceptibility is explained. Three different methods of measuring the linear EO coefficient of a poled nonliner optical polymer thin film are introduced and discussed. All of them make use of the interferometric technique, the difference being in the optical parameters which are interfering.

I. INTRODUCTION

The linear electro-optic (EO) effect is one of the second-order nonliner optical phenomena present in macroscopically noncentrosymmetric materials, where the change in the coefficients of the refractive index ellipsoid is proportional to an external modulating electric field. The linear EO tensor components r_{ij} provide information on the change of refractive indices, and the second-order nonlinear optical (NLO) susceptibilities $\chi^{(2)}_{ijk}(-\omega;\omega,0)$ are obtained from the measurements of r_{ij}. Various material systems were studied as EO material, including inorganic crystals, semiconductors, and organic materials. In particular, organic polymer thin films received wide attention mainly due to their good processibility and intrinsic high bandwidths[1-5]. In the case of polymer thin films doped with NLO molecules, the centrosymmetry of the orientational distribution of the NLO molecules is usually broken by an external dc electric field[6]. The polymer thin film is heated above the glass transition temperature with a poling field applied. The film is then cooled down to room temperature, and the poling field is disconnected. The high viscosity of the glass state of polymer prevents the induced alignment of the molecular dipoles from being randomized. Once the centrosymmetry is broken, the system thus obtained can be viewed as an 'artificial crystal.' From the point group of crystal symmetry, the number of independent linear EO tensors r_{ij} are determined, and the relation between the various components of r_{ij} can be derived.

Experimentally, the nonvanishing components of r_{ij} are measured by an interferometric technique. There are three kinds of interferometry that can be employed to measure r_{ij}, single-beam interferometry, two-beam interferometry, and multiple-beam interferometry. While the single-beam interferometry makes use of the polarization interference of the extraordinary and the ordinary components of the beam passing through the poled, thin-film sample, in the case of two-beam interferometry such as Mach-Zehnder interferometry the phase interference can be achieved selectively. Furthermore, Fabry-Perot interferometry, one kind of multiple-beam interferometry, can also be employed when an increase in interference sensitivity is required. In this paper the index ellipsoid of a poled polymer thin film is analyzed to relate the linear EO tensor r_{ij} with the second-order NLO coefficient $\chi^{(2)}_{ijk}(-\omega;\omega,0)$. Three

interferometric measurement techniques, single-beam, two-beam, and multiple-beam interferometries, are introduced and compared. The advantages and the disadvantages of each technique are analyzed in application to the measurement of EO coefficients in poled polymer thin films.

II. INDEX ELLIPSOID STRUCTURE OF POLED POLYMER THIN FILM

The orientational distribution of NLO chromophores of thermally cured polymer film is isotropic. Hence, the index ellipsoid is a sphere. After electric field poling, the isotropy is broken, and the poled polymer thin film becomes a uniaxial material possessing $C_{\infty v}$ point group symmetry with the infinite-fold symmetry z (optic) axis[7-8]. After the centrosymmetry is broken, the equation of the index ellipsoid becomes

$$\frac{x^2}{n_o^2} + \frac{y^2}{n_o^2} + \frac{z^2}{n_e^2} = 1. \tag{1}$$

When an external modulation field is applied in the z-direction, the changed refractive indices satisfy the same index ellipsoid equation as Eq.(1), only the refractive indices are varied:

$$(\frac{1}{n_o^2} + r_{13}E_z)x^2 + (\frac{1}{n_o^2} + r_{13}E_z)y^2 + (\frac{1}{n_e^2} + r_{33}E_z)z^2 = 1. \tag{2}$$

Changes in the refractive indices are related to the linear EO coefficients, r_{13} and r_{33}, by

$$\Delta n_e = -\frac{1}{2}n_e^3 r_{33}E, \tag{3}$$

$$\Delta n_o = -\frac{1}{2}n_o^3 r_{13}E. \tag{4}$$

On the other hand, the linear EO coefficients r_{ij} are related to the second-order NLO susceptibilities $\chi_{ijk}(-\omega;\omega,0)$ in the following way:

$$r_{ijk} = -\frac{8\pi}{\epsilon_{ii}(\omega)\epsilon_{jj}(\omega)}\chi_{ijk}(-\omega;\omega,0). \tag{5}$$

Now, the macroscopic second-order NLO susceptibilities $\chi_{ijk}(-\omega;\omega,0)$ can be expressed in terms of the molecular hyperpolarizabilities $\beta_{ijk}(-\omega;\omega,0)$ by use of the orientational distribution function of molecular dipoles[9-11]:

$$\chi^{(2)}_{zzz}(-\omega;\omega,0) = N\int \beta_{333}\cos^3(3,z)f(\Omega)d\Omega, \tag{6}$$

$$\chi^{(2)}_{xxz}(-\omega;\omega,0) = N\int \beta_{333}\cos^2(3,x)cos(3,z)f(\Omega)d\Omega. \tag{7}$$

The orientational distribution function $f(\Omega)$ is determined from the minimization of the thermodynamic free energy F of the dipolar interaction of molecular dipoles with an external poling field:

$$F = U - TS \tag{8}$$

where $U = -\mu E\cos\theta$, T is the temperature, and S is the entropy. The minimization of the free energy F yields the following Boltzmann distribution:

$$f(\Omega) = f(\theta) = \sum_{n=0}^{\infty}\frac{2n+1}{2}\frac{i_n(x)}{i_0(x)}P_n(\cos\theta) \tag{9}$$

where $x = \frac{\mu E}{kT}$, $i_n(x)$ are the spherical modified Bessel function, and $P_n(\cos\theta)$ are the Legendre polynomials. After substituting Eq.(9) into Eq.(6) and Eq.(7), the second-order NLO susceptibilities are

$$\chi^{(2)}_{zzz}(-\omega;\omega,0) = N\beta_{333}(-\omega;\omega,0)\frac{1}{5}[3\frac{i_1(x)}{i_0(x)} + 2\frac{i_3(x)}{i_0(x)}], \tag{10}$$

$$\chi^{(2)}_{xxz}(-\omega;\omega,0) = N\beta_{333}(-\omega;\omega,0)\frac{1}{5}[\frac{i_1(x)}{i_0(x)} - \frac{i_3(x)}{i_0(x)}]. \tag{11}$$

Substitution of Eq.(10) and Eq.(11) into Eq.(5) yields the expression of the linear EO coefficients in terms of the microscopic hyperpolarizabilities and the orientational distribution of dipoles.

III. SINGLE-BEAM INTERFEROMETRY

In a poled polymer thin film with $C_{\infty v}$ point group symmetry, two linear EO tensor components, r_{13} and r_{33}, are nonvanishing when the modulation electric-field direction is the same as the poling electric-field direction[12]. Once the relation between r_{13} and r_{33} is known, single-beam interferometry can be employed to measure the linear EO coefficient.

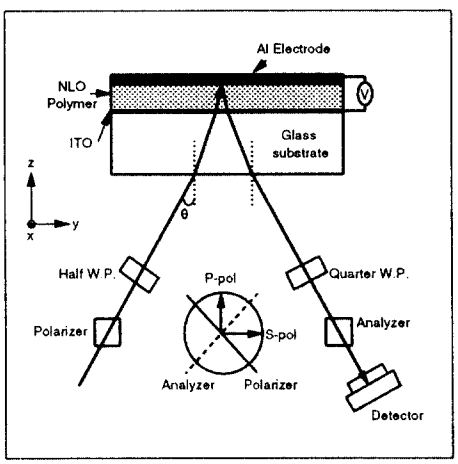

Fig.1. Single-beam polarization interferometry

As shown in Fig.1, the phase modulations experienced by the s-polarized and the p-polarized waves are different. The s-polarized wave picks up the modulation of ordinary wave only. Hence,

$$\Delta n_s = \Delta n_x = -\frac{n_x^3 r_{13} E_z}{2}. \tag{12}$$

In the case of p-polarized light, the electric field of the incident light can be decomposed into the ordinary and the extraordinary wave components. The refractive index, $n_p(\theta)$, of the p-polarized light with the incident angle θ satisfies the following equation:

$$\frac{1}{n_p^2(\theta)} = \frac{\cos^2\theta}{n_y^2} + \frac{\sin^2\theta}{n_z^2}. \tag{13}$$

The change in the refractive index due to the EO modulation is, therefore,

$$\Delta n_p \approx \Delta n_y \cos^2\theta + \Delta n_z \sin^2\theta. \tag{14}$$

The optical phase difference between the s- and the p-polarized light, Γ, is simply given by

$$\Gamma = \Delta\phi_s - \Delta\phi_p \approx -\frac{\omega}{c}\frac{n_o^3 E_z L}{2}(r_{13} - r_{33})\sin^2\theta. \tag{15}$$

From the given orientational distribution function, a relation between r_{13} and r_{33} can be obtained. With that relation, Eq.(15) gives the linear EO coefficient that can be measured by a simple experimental setup as shown in Fig.2.

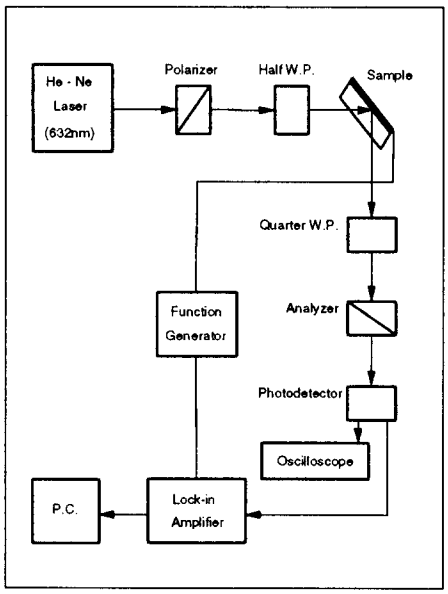

Fig.2. Schematic diagram of the experimental setup

IV. TWO-BEAM INTERFEROMETRY

Mach-Zehnder (MZ) interferometry is one kind of two-beam interferometry in which the amplitude of the incident beam is split. Heterodyne MZ interferometry is a variation of MZ interferometry. In the former, the incident beam is split into a reference arm (local oscillator) and a frequency-shifted sample arm[13]. The reference and the sample arms are recombined by a dielectric mirror, and the spectrum of the combined beam is analyzed through a spectrum analyzer to identify any frequency shift induced in the sample arm. At the detector, the photocurrent is given by

$$i(t) = I_{LO} + I_S + 2\sqrt{I_{LO} I_S}\cos[\omega_{LO} t + \Delta\phi(t)] \tag{16}$$

where I_{LO} and I_S are the dc currents due to the reference- and the sample-arm beams, respectively, and $\Delta\phi(t)$ is the time-dependent linear EO phase shift. For a sinusoidal modulation voltage and double-pass beam, we get

$$\Delta\phi(t) = 2\pi r_{13} n^3 \frac{L}{\lambda} E_m \sin(\omega_m t) = \delta \sin(\omega_m t) \tag{17}$$

where λ is the free-space wavelength of the laser light, $E_m \sin(\omega_m t)$ is the modulation E field, and L is the active sample thickness. Expanding Eq.(16), we obtain a relation between the photocurrents of the n-th harmonics:

$$\frac{i[(\omega_{LO} \pm n\omega_m)t]}{i(\omega_{LO} t)} = \frac{J_n(\delta)}{J_0(\delta)} \tag{18}$$

where $J_n(\delta)$ is the n-th order Bessel function. For small modulations, the ratio of $J_1(\delta)$ to $J_0(\delta)$ is approximately $\delta/2$. This means that a measurement of the photocurrent heights at the spectrum analyzer gives the linear EO coefficient r_{13}. When compared with single-beam interferometry, one advantage of MZ interferometry is that the independent determination of r_{13} is possible.

V. MULTIPLE-BEAM INTERFEROMETRY

For multiple interference, the transmission T of a Fabry-Perot (FP) interferometer with two mirrors is expressed as

$$T = \frac{I}{1 + F_e \sin^2 \delta} \tag{19}$$

where $I = \frac{T_e^2}{(1-R_e)^2}$ is the effective transmission, and $\delta = \frac{2\pi nl}{\lambda}\frac{1}{\cos\theta_s}$ is the optical phase inside the interferometer. (l is the thickness of the space layer, n the refractive index of the space materials, and θ_s the refractive angle in the space layer.) The refractive angle θ_s is related to the incident angle θ through Snell's law, $n \sin\theta_s = \sin\theta$.

When an external electric-field modulation is applied between the two metal electrode mirrors, the linear EO effect present inside the film layer of an FP etalon induces an optical phase change. The derivative of the transmission, dT, is

$$dT = (\frac{\partial T}{\partial n})_l dn = \frac{2\pi nl}{\lambda} \frac{IF_e \sin 2\delta}{(1 + F_e \sin^2 \delta)^2} \frac{(n^2 - 2\sin^2\theta)}{(n^3 - n\sin^2\theta)} dn. \tag{20}$$

Here, the change in the refractive index dn can be related with the linear EO coefficient. A film poled in the direction of the etalon surface normal will have two nonvanishing electro-optic coefficients, r_{13} and r_{33}. An electric field applied in the direction of the surface normal will result in a change in the index of refraction, as observed by TE-polarized light, given by

$$dn_{TE} = dn_y = -\frac{1}{2} n_o^3 r_{13} dE_z \tag{21}$$

where n_o is the ordinary refractive index. The differential change in the effective index, as experienced by TM-polarized light, is related to the applied field by

$$dn_{TM} = dn_{eff} = -\frac{n_{eff}^3}{2}(r_{13}\cos^2\theta_s + r_{33}\sin^2\theta_s) dE_z \tag{22}$$

where n_{eff} is the effective index, which can be determined by the relation

$$\frac{1}{n_{eff}^2(\theta)} = \frac{\cos^2\theta_s}{n_o^2} + \frac{\sin^2\theta_s}{n_e^2} \tag{23}$$

where n_o and n_e are the ordinary and extraordinary indices, respectively.

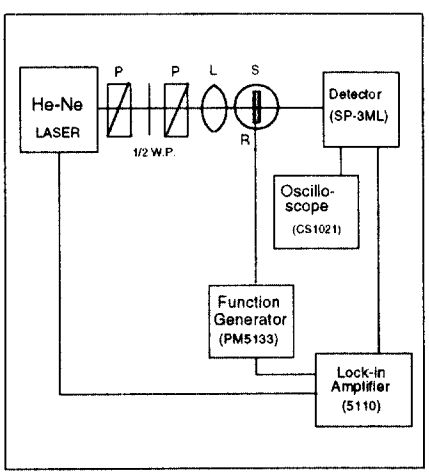

Fig.3. Schematic diagram of the experimental setup

Substitution of Eqs.(22) and (23) into Eq.(20) yields the relation between the linear EO coefficients and the transmission modulation. Here, we note that the TE-polarized light measurement provides an independent determination of r_{13} as shon in Eq.(21). Another advantage of FP interferometry is the stability of its interference pattern compared with that of MZ interferometry. In an etalon structure, the fixed spacing of the two mirrors provides a mechanical stability essential to a stable interferometer.

Experimentally, the optical phase change is achieved by rotating the thin film sample in a rotation stage. Variation in the incident angle of the laser light induces an optical-path-length change inside the film, which results in a change of an optical phase. (See Fig.3). Examples of the experimental data are shown in Fig.4 and Fig.5. The linear dependence of the modulated output confirms that the modulation is due to the linear EO effect. From Fig.5 we find that the point where the transmission modulation is maximum agrees with that where the differential transmission is maximum, as shown in Eq.(20).

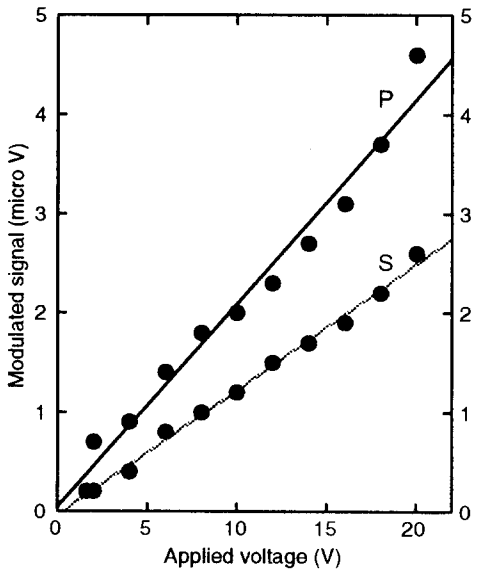

Fig.4. The modulation output as a function of the ac modulation voltage

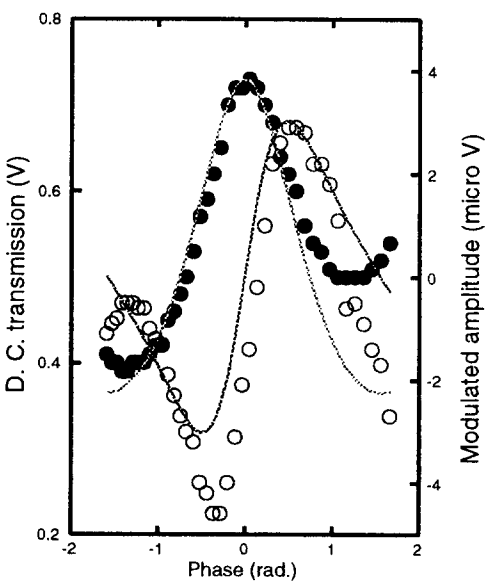

Fig.5. The intensity of the interfering light and the modulation amplitude

VI. CONCLUSION

Three interferometric techniques are introduced for measuring the linear EO coefficients in poled polymer thin films. Single-beam interferometry makes use of polarization interference between the ordinary and the extraordinary waves. A two-beam interferometer, introduced here as the heterodyne Mach-Zehnder interferometer, utilizes the standard reference- and sample-arm configuration. The heterodyne technique is useful for a dynamic study of the linear EO response. Fabry-Perot interferometry, as one example of multiple interferometry, has other advantages, such as the stability of the interference pattern and the ability to independently determine the linear EO coefficient.

ACKNOWLEDGMENTS

This work is supported by the Korea Science and Engineering Foundation (Grant No. 95-0300-06-01-3) and by the Basic Science Research Institute Program, Ministry of Education, Republic of Korea (Grant No. BSRI-97-2428).

REFERENCES

[1] J. I. Thackara, G. F. Lipscomb, M. A. Stiller, A. J. Ticknor, and R. Lytel, Appl. Phys. Lett.**52**, 1031 (1988).

[2] T. E. VanEck, A. J. Ticknor, R. S. Lytel, and G. F. Lipscomb, Appl. Phys. Lett.**58**, 1558 (1991).

[3] D. G. Girton, S. Kwiatkowski, G. F. Lipscomb, and R. Lytel, Appl. Phys. Lett.**58**, 1730 (1991).

[4] C. C. Teng, Appl. Phys. Lett.**60**, 1538 (1992).

[5] C. K. L. Wah, K. Iizuka, and A. P. Freundorfer, Appl. Phys. Lett.**63**, 3110 (1993).

[6] K. D. Singer, M. G. Kuzyk, W. R. Holland, J. E. Sohn, S. J. Lalama, R. B. Comizzoli, H. E. Katz, and M. L. Schilling, Appl. Phys. Lett.**53**, 1800 (1988).

[7] A. Yariv, *Quantum Electronics*, 3rd. ed. (Wiley, New York, 1988).

[8] K. D. Singer, M. G. Kuzyk, and J. E. Sohn, J. Opt. Soc. Am.**B4**, 968 (1987).

[9] J. W. Wu, J. Opt. Soc. Am.**B8**, 142 (1991).

[10] Y. R. Shen, *The Principles of Nonliner Optics* (Wiley, New York, 1984).

[11] P. N. Butcher and D. Cotter, *The Elements of Nonlinear Optics* (Cambridge University Press, Cambridge, 1990).

[12] C. C. Teng and H. T. Man, Appl. Phys. Lett.**56**, 1734 (1990).

[13] J. F. Valley, J. W. Wu, and C. L. Valencia, Appl. Phys. Lett.**57**, 1084 (1990).